Journal of Nuclear Materials 62 (1976) 229–239

PRECIPITATION IN ZIRCONIUM-NIOBIUM MARTENSITES *

S. BANERJEE, S.J. VIJAYAKAR and R. KRISHNAN
Metallurgy Division, Bhabha Atomic Research Centre, Trombay, Bombay-400 085

Received 16 March 1976

The structure of Zr-2.3%Nb and Zr-5.5%Nb alloy martensites on tempering at different temperatures in the range of 350 to 600°C was studied by optical and transmission electron microscopy. The equilibrium β-niobium phase (β_2) was found to be the precipitating phase on tempering the Zr-2.3%Nb martensites at temperatures up to 500°C and the Zr-5.5% Nb martensites at temperatures upto 450°C. Precipitation of the metastable β_1 phase of the monotectoid composition (Zr-20%Nb) was observed to occur on tempering the Zr-2.3%Nb alloy at 550 and 600°C and the Zr-5.5%Nb alloy at 500 and 550°C. On tempering the latter alloy at 600°C, the martensite was found to revert back to the supersaturated β phase, which subsequently decomposed into a mixture of the α and the β_1 phases. These observations have been explained on the basis of hypothetical free energy versus composition diagrams. The orientation relation of the β_1 precipitates with respect to the α phase was found to be as follows: $(0001)_\alpha \parallel \{011\}_{\beta_1}$; $\langle 11\bar{2}0\rangle_\alpha \parallel \langle 1\bar{1}1\rangle_{\beta_1}$. It was also seen that a β_1 precipitate forming at a twin boundary maintains equivalent orientation relations with the two adjacent twin related portions.

La structure des martensites des alliages Zr-2,3% Nb et Zr-5,5% Nb après revenu à différentes températures dans l'intervalle 350–600°C a été étudiée par microscopie optique et électronique. La phase d'équilibre β-niobium (β_2) a été trouvée comme étant la phase précipitant au cours du revenu des martensites de Zr-2,3% Nb aux températures atteignant 500°C et les martensites de Zr-5,5% Nb aux températures allant jusqu'à 450°C. La précipitation de la phase β_1 métastable de composition monotectoïde (Zr-20% Nb) s'est révélée se produire par revenu de l'alliage Zr-2,3% Nb à 500 et 600°C et de l'alliage Zr-5,5% Nb à 500 et 550°C. Par revenu du dernier alliage à 600°C, la martensite subit sa réversion en la phase β sursaturée, qui se décompose ultérieurement en un mélange des phases α et β_1. Ces observations sont expliquées en se basant sur les diagrammes hypothétiques d'énergie libre en fonction de la composition. La relation d'orientation des précipités β_1 par rapport à la phase α s'est révélée être la suivante: $(0001)_\alpha \parallel \{011\}_{\beta_1}$; $\langle 11\bar{2}0\rangle_\alpha \parallel \langle 1\bar{1}1\rangle_{\beta_1}$. Il a été également observé qu'un précipité β_1 se formant sur un joint de macle maintient des relations d'orientation équivalentes avec les deux portions de macle adjacentes.

Die Struktur der Zr-2,3% Nb- und Zr-5,5% Nb-Martensite während der Wärmebehandlung bei verschiedenen Temperaturen zwischen 350 und 600°C wurde licht- und transmissionselektronenmikroskopisch untersucht. Nach den Beobachtungen ist die β-Nb-Gleichgewichtsphase β_2 die sich ausscheidende Phase während der Wärmebehandlung des Zr-2,5% Nb-Martensits bis zu 500°C und des Zr-5,5% Nb-Martensits bis zu 450°C. Die Ausscheidung der metastabilen β_1-Phase in der monotektoiden Zusammensetzung (Zr-20% Nb) tritt während der Wärmebehandlung der Zr-2,3% Nb-Legierung zwischen 550 und 600°C und der Zr-5,5% Nb Legierung zwischen 500 und 550°C auf. Während der Wärmebehandlung der letzteren Legierung bei 600°C erfolgt eine Rückumwandlung des Martensits in die übersättigte β-Phase, die anschliessend ein Gemisch aus der α- und β_1-Phase zerfällt. Diese Beobachtungen werden mit dem hypothetischen Diagramm der freien Energie in Abhängigkeit von der Zusammensetzung erklärt. Die Orientierungsbeziehungen der auf die α-Phase bezogenen β_1-Ausscheidungen lauten: $(0001)_\alpha \parallel \{011\}_{\beta_1}$; $\langle 11\bar{2}0\rangle_\alpha \parallel \langle 1\bar{1}1\rangle_{\beta_1}$. Es wurde ferner beobachtet, dass eine β_1-Ausscheidung, die an einer Zwillingsgrenze entsteht, die äquivalenten Orientierungsbeziehungen mit den beiden Grössen des angrenzenden Zwillings beibehält.

* This forms a part of the Ph. D thesis submitted by S. Banerjee to the Indian Institute of Technology, Kharagpur in September, 1973.

1. Introduction

Zirconium-2.5 percent * niobium alloy is increasingly being used as a material for pressure tubes in nuclear reactors. The heat-treatment used for strengthening this alloy involves quenching from the ($\alpha + \beta$) phase field followed by tempering at 500°C. The microstructural changes that occur during the tempering of Zr-2.5% Nb alloys have already been investigated by Williams and Gilbert [1] and by Sabol [2] using the transmission electron microscopic (TEM) technique. It has been reported that the equilibrium beta niobium phase is precipitated during tempering at temperatures ranging from 400 to 600°C. A similar observation has been made by Heheman [3] on Zr-5% Nb alloy. This paper reports some new results obtained during the course of a study of the precipitation behaviour in Zr-2.3% Nb and Zr-5.5% Nb alloys. The latter alloy was chosen because the solution heat treatment in the ($\alpha + \beta$) phase field, as practised industrially, enriches the β phase of the Zr-2.5% Nb alloy to about 5 to 6% niobium content.

2. Experimental

Alloys were prepared from iodide purity zirconium and high purity niobium by electron beam melting. The homogenized buttons were cold rolled to about 0.2 mm. thick strips without any intermediate annealing. Samples for heat treatment were sealed in evacuated silica capsules back-filled with helium. The solutionizing treatment was carried out in the β phase field (at 1000° C) for 15 min followed by quenching in water. Tempering was carried out at 350, 450, 500, 550 and 600°C for periods of 10, 100, 1000 and 10000 min. Specimens for TEM investigations were chemically polished in a solution containing 5 parts HF, 45 parts HNO_3 and 50 parts water and subsequently electropolished at −50°C in a solution containing 6 parts perchloric acid, 34 parts n-butanol and 60 parts methanol.

* All compositions are given in weight percent.

3. Results

3.1. Zr-2.3% Nb alloy

3.1.1. Optical microscopic observations

The structure of the samples tempered at temperatures up to 500°C was not distinguishable from that of the as-quenched martensite, even for tempering times of 10 000 min. but precipitates could easily be detected in samples tempered at 550 and 600° C. The volume fraction of the precipitate phase (14%) as measured by the point count method was found to be much more than that expected from the phase diagram, suggesting that this was not the equilibrium beta niobium phase (denoted by β_2) but was of a composition relatively less enriched in niobium. The accuracy in the estimation of the volume fraction of such fine precipitates is expected to be poor due to the formation of etching artifacts. In view of this, the volume fraction was also measured quantitatively from TEM observations as described later.

3.1.2. TEM observations

The precipitation process was found to be extremely sluggish at temperatures lower than 500°C. The presence of very fine precipitates could be detected only in the samples tempered at 450°C for 1000 min. or more. The fine dispersion and the small volume fraction of this precipitated phase precluded its identification by X-ray or electron diffraction.

At 500°C, the precipitation reaction was found to be relatively faster. Tempering for 100 minutes at this

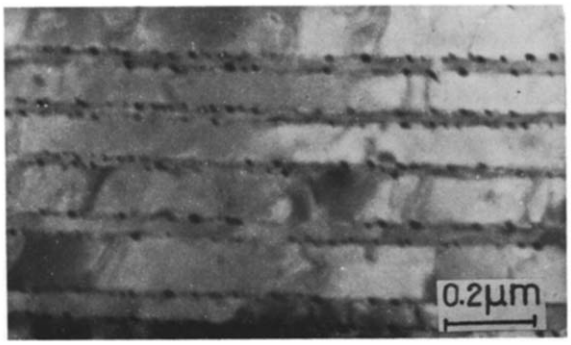

Fig. 1. Zr-2.3% Nb, beta quenched, tempered at 500°C for 100 min. The micrograph shows a distribution of fine precipitates along the twin boundaries. No matrix precipitate is visible.

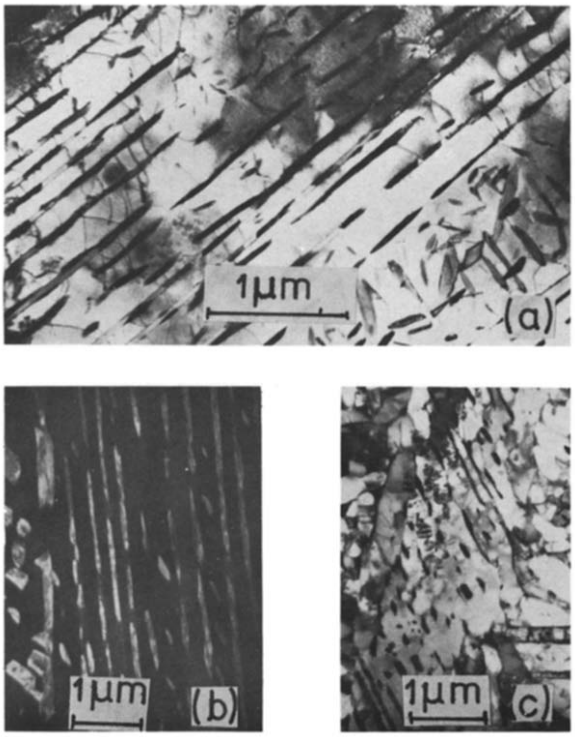

Fig. 2. Zr-2.3%Nb, beta quenched, tempered at 600°C for 10 min. (a) shows β_1 precipitates along the twins which are partially annihilated. On the left hand side of this micrograph, all precipitate plates are confined to the twin interfaces which are oriented normal to the foil plane. The volume fraction of the precipitate phase in this region has been found to be 13%. (b) is a $\{110\}\beta_1$ dark field micrograph showing a lamellar distribution of the precipitates, volume fraction of the 'edge on' precipitates being 18%. (c) shows complete removal of internal twins.

temperature produced clearly resolvable precipitates along the twin boundaries (fig. 1) while precipitation in the matrix was observed only occasionally. Analyses of the SAD patterns revealed the precipitate phase to be the niobium rich β_2 phase. This is in conformity with the phase diagram of the Zr-Nb system [4,5] and with the previous TEM investigations [1,2].

In the samples tempered at 550°C and at 600°C, the average volume fraction of the precipitate phase as measured from the regions where precipitate plates were normal to the foil plane, was found to be about 15% (fig. 2). In order to identify the precipitate phase, SAD from thin foils and X-ray diffraction from bulk samples were taken. Analyses of the results indicated that the precipitate phase has a bcc structure with a lattice parameter of 3.52 Å which is significantly different from the lattice parameter (3.34 Å) of the β_2 phase [6,7]. This value of the lattice parameter matches that of the zirconium rich beta phase (denoted by β_1) close to the monotectoid composition. Moreover, this observation agrees well with the fact that the volume fraction of the precipitates as obtained from both the optical and the electron microscopic observations was fairly close to that predicted (10%) by construction of the tie line between the α and the β_1 phases.

In addition to the precipitation of a second phase, annihilation of internal twins was noticed in the samples tempered at 550 and 600°C. In many regions, internal twins were found to shrink or completely disappear leaving behind either a discontinuous array of precipitates along the "ghost" (pre-existing) twin boundaries or a set of parallel lamellae of the precipitate phase which appeared to have grown at the expense of the twin portion of the martensite plate (fig. 2). A similar observation has been made in the case of Ti-Ta alloys by Bywater and Christian [8].

3.2. Zr-5.5% Nb alloy

3.2.1. Optical microscopic observations

These observations were similar to those made on the Zr-2.3% Nb alloy except for samples tempered at 600°C. The typical structure produced on tempering

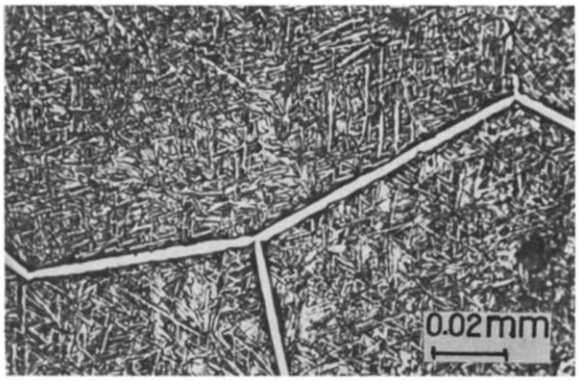

Fig. 3. Zr-5.5% Nb, beta quenched, tempered at 600°C for 1000 min. The micrograph shows that the light etching phase (α) is distributed in a Widmanstatten pattern in the matrix (β). At the grain boundaries of the beta phase, a thick band of the light etching phase is seen sandwiched between regions of the dark etching phase.

the Zr-5.5% Nb alloy at 600°C (fig. 3) shows the major phase (light etching) distributed in a Widmanstatten pattern in a matrix of the minor (dark etching) phase. A thick grain boundary region consisting of a band of the major phase sandwiched between regions of the minor phase is also seen. The major and the minor phases were identified as α-zirconium and β_1 respectively by X-ray diffraction. From the relative intensities of the X-ray diffraction peaks corresponding to the $(0002)_\alpha$ and the $\{110\}_{\beta_1}$ reflections, a quantitative estimation of the weight fraction ratio of these two phases was made. Since the texture co-efficient of the $(0002)_\alpha$ reflection was close to unity, the inaccuracy caused by the texture effect is not expected to be very significant. It was seen that the ratio of the weight fractions of the β_1 and the α phases was close to 1 : 3, a value predicted from the construction of a tie line joining the α and the β_1 phases.

The samples tempered at 550 and 500°C showed precipitates which could be resolved under the optical microscope. Morphologically these structures were similar to that of the Zr-2.3% Nb martensite tempered at 550 and 600°C. No precipitates could be detected in samples tempered at lower temperatures.

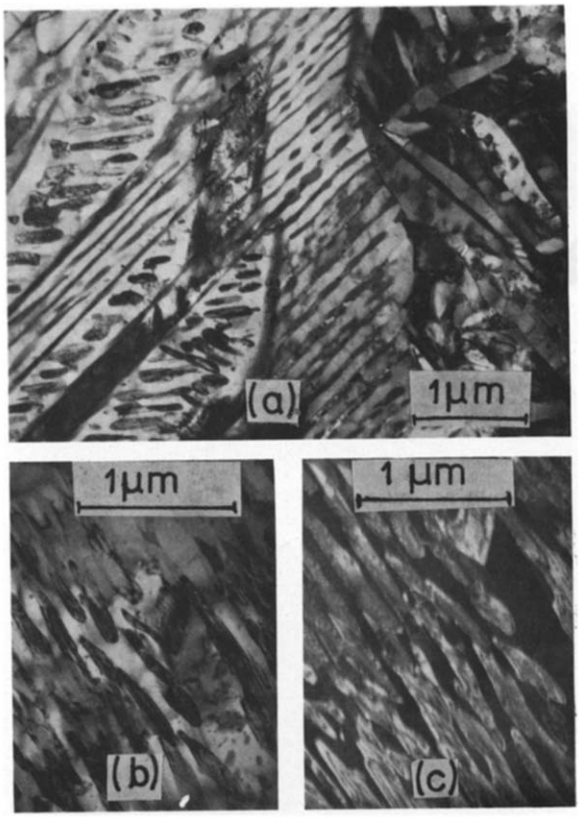

Fig. 4. Zr-5.5% Nb, beta quenched, tempered at 550°C for 100 min. (a) shows extensive precipitation of the β_1 phase at the twin and the plate interfaces as well as within the matrix. (b) and (c) are the bright and dark field ($(110)_{\beta_1}$ reflection) micrographs showing a large volume fraction of the β_1 phase.

3.2.2. TEM observations

As in the case of the Zr-2.3% Nb alloy, TEM observations on samples tempered at 450°C and below showed extremely fine β_2 precipitates, while extensive precipitation of the β_1 phase was noticed in samples tempered at 500 and 550°C. Precipitation in the matrix as well as along the interfaces was found to occur to a larger extent than in the Zr-2.3% Nb alloy (fig. 4).

Samples tempered at 600°C for a period of 100 minutes or more revealed that the Widmanstatten plates (major constituent) in the two phase structure of these samples were of the α phase and were distributed in a continuous matrix of the β_1 phase (minor constituent) (fig. 5). These metallographic features, revealed by optical and electron microscopy observations, suggest that the α phase was precipitated in the β_1 matrix, which appeared to have originated by a reversion process. This is supported by the observations made on samples tempered at 600°C for a short time, within which, the reversion of the martensitic α′ phase to the supersaturated β phase was not complete. At several places α′ plates were found to be partly con-

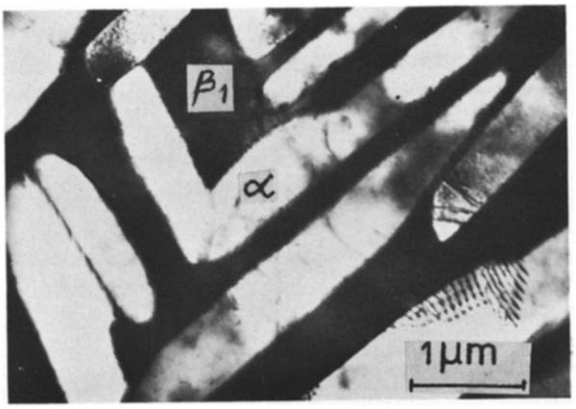

Fig. 5. Zr-5.5% Nb, beta quenched, tempered at 600°C for 1000 min. The morphology shows a distribution of alpha plates in a continuous matrix of the β_1 phase.

sumed by the advancing β phase boundaries. Subsequent to the reversion, the newly formed supersaturated β phase decomposed into a mixture of the α and the metastable β_1 phases.

3.3. Matrix-precipitate orientation relationship

The orientation relations in the case of the twin boundary precipitates were determined from SAD pat-

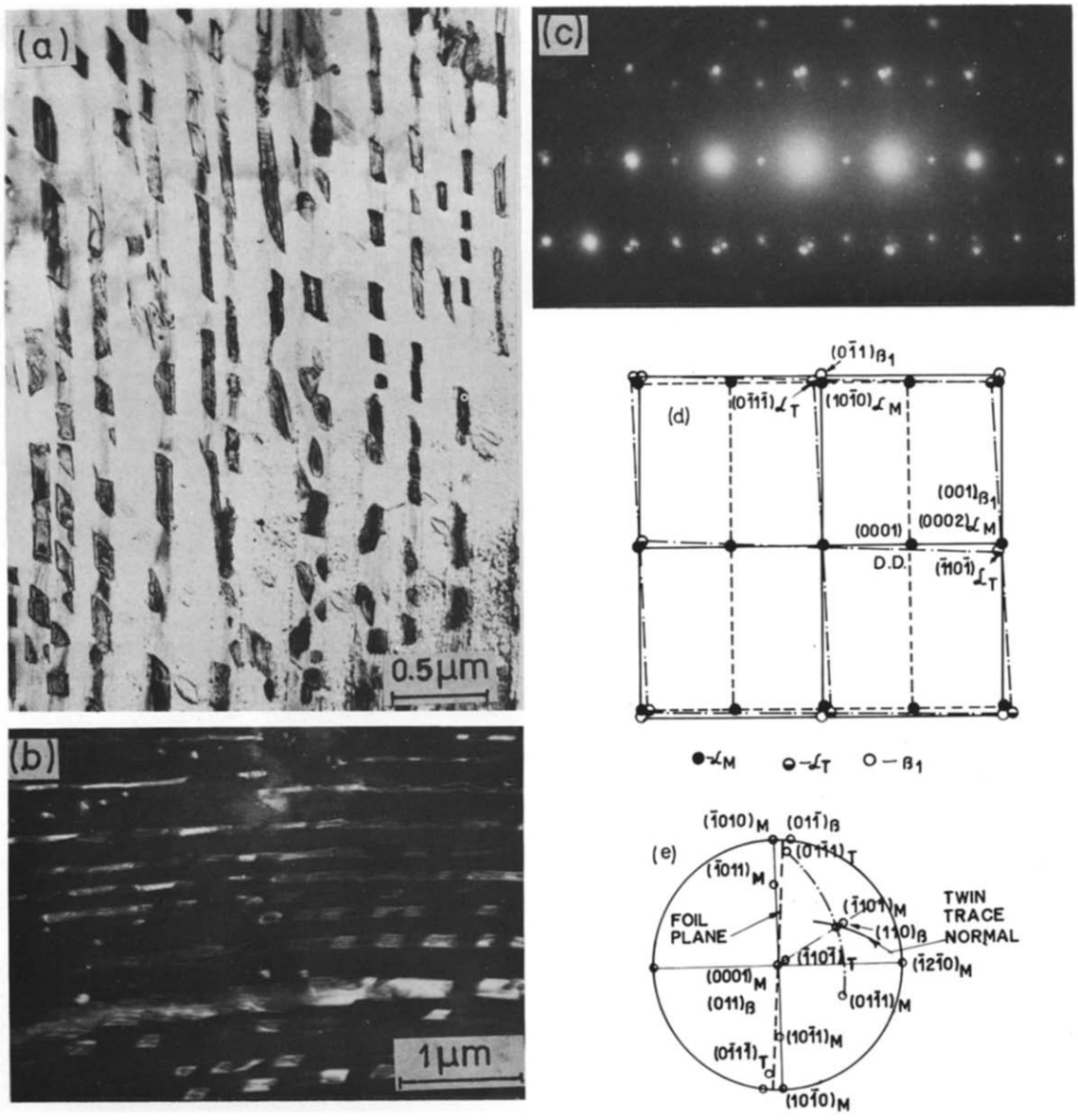

Fig. 6. Zr-2.3% Nb, beta quenched tempered at 600°C for 10 min. The bright field micrograph (a) shows a distribution of plate shaped precipitates along the twin interfaces. The dark field micrograph (b) is obtained by imaging $(0\bar{1}1)_{\beta_1}$ reflection. The SAD pattern and its key ((c) and (d) respectively) show a superimposition of three reciprocal lattice sections. The stereographic projection (e) represents the relative orientations of the pair of twin related α crystals and of the β_1 precipitates. The $(\bar{1}10)_{\beta_1}$ plane is seen to be parallel to the $(\bar{1}101)$ twin plane.

terns taken from regions containing these precipitates. These patterns consisted of three superimposed reciprocal lattice sections, corresponding to the precipitate crystal and to a pair of twin-related α crystals. Fig. 6 shows a typical SAD pattern from which the orientations of the β_1 precipitate and of the two twin related α crystals were determined. Orientations of all the three crystals were drawn on the stereogram with the $(0001)_{\alpha_M}$ plane (basal plane of the major twin component of the α phase) as the plane of projection. The orientation relation between the major twin component (α_M) and the precipitate could be expressed as follows:

$$(0001)_{\alpha_M} \| (011)_{\beta_1} ; [11\bar{2}0]_{\alpha_M} \| [1\bar{1}1]_{\beta_1} ;$$

a typical Burgers' [9] relation for the bcc $\rightleftharpoons$ hcp transformation. It was also seen that the orientation of the minor twin component (α_T) could be obtained by reflecting the poles corresponding to the major twin on the $(\bar{1}101)_{\alpha_M}$ plane, suggesting that twinning was along the $\bar{1}101$) plane. This was confirmed by single surface trace analysis of the composition plane of the twin. It could also be seen from the stereogram that the precipitate maintains an approximately equivalent orientation relationship with the minor twin component (α_T) as described in the following:

$$(0001)_{\alpha_T} \| (10\bar{1}\bar{1})_{\beta_1} ; [11\bar{2}0]_{\alpha_T} \| [\bar{1}1\bar{1}]_{\beta_1}$$

This was also evident from the fact that the $(\bar{1}101)$ twin plane was approximately parallel to a $\{110\}$ type mirror plane of the β_1 crystal.

The orientation relation between the homogeneously nucleated β_1 precipitates and the matrix α was found to be the same and this is illustrated in fig. 7.

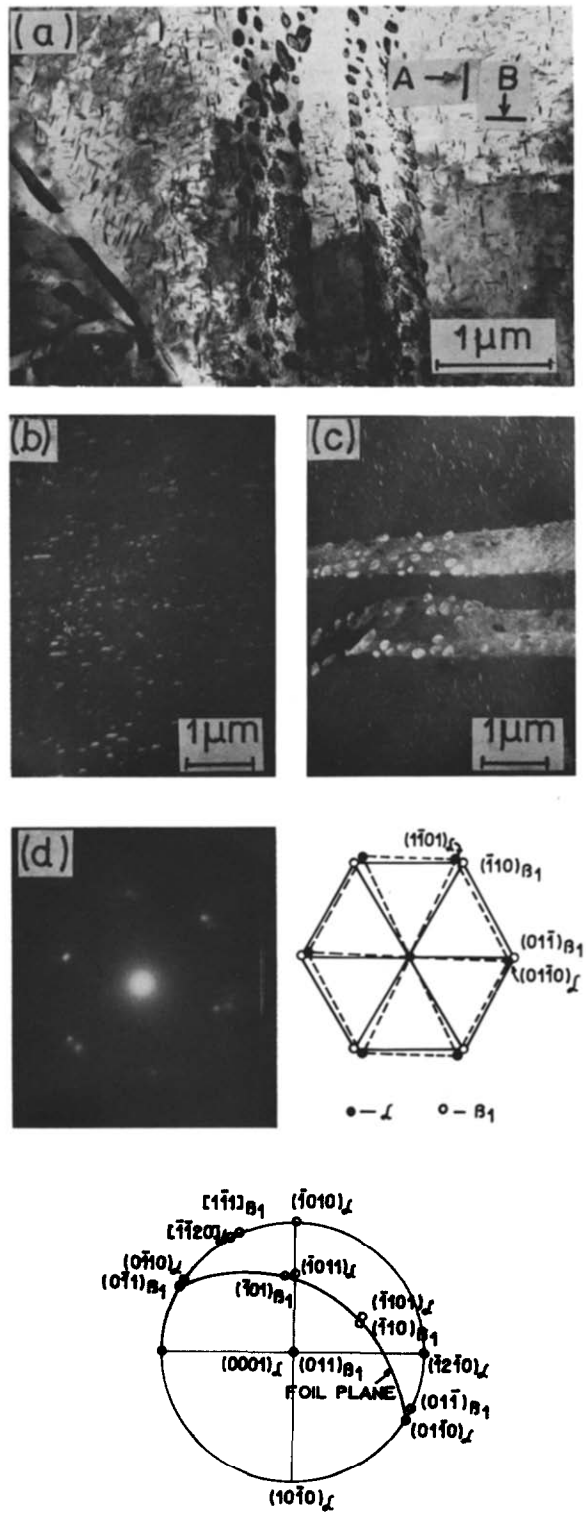

Fig. 7. Zr-2.3% Nb, beta quenched, tempered at 550°C for 100 min. Bright field micrograph in (a) shows fine needle like precipitates along several directions. In addition coarse precipitates are seen along the twin interfaces. The dark field micrographs (b) and (c) show bright contrast from sets of precipitates marked A and B respectively. In both cases the imaging reflections were of $\{110\}_{\beta_1}$ type. The corresponding SAD pattern and the key are given in (d) and (e). The stereographic projection in (f) shows the orientation relation between the 'A' precipitates and the matrix. The 'B' precipitates and the twin boundary precipitates follow identical variant of orientation relation.

4. Discussion

4.1. Precipitation reactions

The present experimental observations can be summarised as follows:

(i) During the tempering of the Zr-2.3% Nb and the Zr-5.5% Nb alloys at temperatures up to 500 and 450°C respectively, the β_2 phase was found to be precipitated.

(ii) the precipitation of the β_1 phase was found to occur in Zr-2.3% Nb, tempered at 550 and 600°C and in Zr-5.5% Nb tempered at 500 and 550°C.

(iii) On tempering the Zr-5.5% Nb alloy at 600°C, the supersaturated α' phase reverted back into a supersaturated β phase which subsequently decomposed into a mixture of the α and the β_1 phases.

These observations can be rationalised on the basis of hypothetical free energy-composition diagrams. At the monotectoid temperature (610°C), β_1 is in equilibrium with a mixture of α and β_2. The miscibility gap in the β phase at temperatures above the monotectoid is suggestive of a maximum in the free energy-composition curve for the β phase. In fact, experimental evidence for the occurrence of a spinodal decomposition in β-Zr-Nb alloys at temperatures above and below the monotectoid temperature have recently been provided by Flewitt [10]. The hypothetical free energy-composition diagram for 600°C is shown in fig. 8(a) in which the free energies of the supersaturated martensites (α') of the Zr-2.3% Nb and the Zr-5.5% Nb alloys are represented by the points A and B respectively. The G_α and the G_β curves are made to intersect at a point D corresponding to a composition represented by X_d. This means that for the alloy composition X_d, 600°C is the temperature, T_0, at which the free energies of the α and the β phases are equal. From Kaufman's work [11] it is known that the temperature T_0 is usually about 50°C higher than the M_s temperature for zirconium and titanium base alloys. Thus a rough estimate of values of T_0 for the present alloys can be made from known M_s temperatures [12]. For Zr-5.5% Nb, the temperature T_0 turns out to be about 580°C and so the composition X_d will correspond to a value which is slightly lower than 5.5% Nb. Hence, a reversion of the Zr-5.5% Nb alloy from the α' phase to the supersaturated β phase will be possible at 600°C and the driving force for such a reaction is given by $\Delta G_{BB'}$. This supersaturated β phase subsequently transformed into a metastable structure containing the α phase distributed in a Widmanstatten pattern within the β_1 matrix. The free energy of the mixture of the α and the β_1 phases is represented by the point B''. Though the most stable configuration (represented by B''') corresponds to a mixture of the α and the β_2 phases, a transformation leading to the formation of $(\alpha + \beta_2)$ was not found to occur at 600°C even after 10 000 min of tempering.

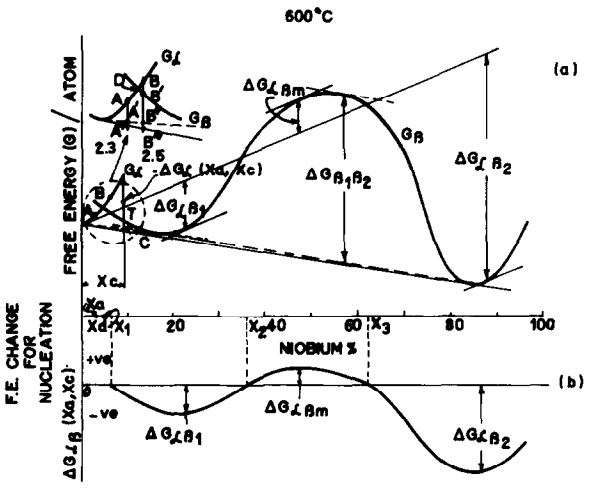

Fig. 8. (a) Hypothetical free energy-composition diagram at 600°C. (b) Free energy change for nucleation versus composition of the nucleus as derived from fig. 8(a).

The process of tempering at 600°C was found to be entirely different for the Zr-2.3% Nb alloy. The temperature T_0 for this alloy is much higher than 600°C and consequently a reversion into the β phase is not possible. In this case, the excess solute atoms were thrown out of the α' lattice to form precipitates. Precipitation could take place in either of the following ways depending on the magnitudes of the driving and the restraining forces for the respective precipitation reactions.

(i) Supersaturated $\alpha' \rightarrow \alpha + \beta_1$

(ii) Supersaturated $\alpha' \rightarrow \alpha + \beta_2$

At 600°C, $\Delta G_{AA'}$, the net driving force for reaction (i) would be smaller than $\Delta G_{AA''}$, that for reaction

(ii), only by a marginal extent. But these changes in free energy per atom of the whole assembly do not represent the driving forces for the initial nucleation of the β_1 and the β_2 precipitates. When a small β nucleus corresponding to a composition X_c forms in an α' matrix of composition X_a, the matrix remains essentially unchanged in composition and the free energy change for nucleation per atom of the β-nucleus is given by TC where TC is the vertical distance between the free energy curve of the β phase and the tangent to the curve of the α phase at A. If $\Delta G_{\alpha\beta}(X_a, X_c)$, the change in free energy per atom of the nucleus is plotted as a function of the composition of the nucleus, one can see that the two minima corresponding to the formation of the β_1 and the β_2 precipitates are separated by a maximum. It is also to be noted that $\Delta G_{\alpha\beta_1}$ is much smaller than $\Delta G_{\alpha\beta_2}$, the maximum driving forces for the nucleation of the β_1 and the β_2 precipitates respectively. Thus from the consideration of the driving force for nucleation, one would expect that the nucleation of the β_2 precipitates would be more favoured. However, this is contrary to the experimental observations. In order to explain this discrepancy, one should also consider factors like the size barrier and the composition barrier which tend to inhibit the formation of a precipitate nucleus. It can be seen from the $\Delta G_{\alpha\beta}(X_a, X_c)$ versus composition diagram (fig. 8(b)) that the nucleation of the β phase can occur only when the composition of the nucleus lies within any of the following two ranges:

$$X_1 < X_c < X_2, \qquad X_c > X_3$$

Nucleation of both β_1 and β_2 precipitates essentially involves two processes: (i) a segregation of niobium atoms and (ii) a transformation from the hcp to the bcc structure. Whether the process of niobium enrichment would precede or follow the nucleation of the β phase would be determined by the relative magnitudes of ΔG_c and $n_c \Delta G_\alpha (X_a, X_c)$, where ΔG_c is the activation energy necessary for the formation of the interface of a critical nucleus of composition X_c, containing n_c number of atoms and $n_c \Delta G_\alpha (X_a, X_c)$ corresponds to the free energy increase accompanying the formation of an α-segregate of composition X_c [13, 14]. It is evident that the magnitude of $\Delta G_\alpha (X_a, X_c)$ would be extremely large for $X_c > X_3$ and thus a segregation in the α phase to this extent would correspond to a very large potential barrier. The only alternative mode of β_2 nucleation would then consist of the formation of β-nuclei having compositions in the range $X_1 < X_c < X_2$ and a subsequent enrichment of these nuclei with niobium atoms. But the latter process would again involve a large free energy barrier as shown in fig. 8(a). In contrast, the free energy of a nucleus in this range of composition drops continuously as its composition approaches that of a β_1 precipitate.

In addition to this free energy barrier associated with compositional fluctuations, energy must also be supplied to form the precipitate-matrix interface in the case of a non-coherent nucleus or to provide for the strain associated with the formation of a coherent precipitate. This surface energy is again constituted of two components, one resulting from the structural and the other from the compositional dissimilarities across the interface. The magnitude of the compositional part has been shown to be proportional to $(\Delta X)^2$, where ΔX is the difference in the solute concentrations of the matrix and the precipitate [15]. Therefore, considering this part of the surface energy, the requirement would be more for the β_2 than for the β_1 precipitates. The other part of the surface energy as well as the strain energy are essentially dependent on the degree of structural disregistry at the interface. The requirement with respect to these would also be more for a β_2 nucleus for which the misfit at the adjoining $\{10\bar{1}1\}_\alpha$ and $\{110\}_\beta$ planes is larger than that for a β_1 nucleus (as shown in the next section). Thus the overall size barrier associated with the nucleation of the β_2 phase would be larger than that in the case of the β_1 phase.

In view of the preceding discussions it is evident why the nucleation of the β_1 phase is favoured in preference to that of the β_2 phase, even though the driving force for the nucleation of the former is much smaller than

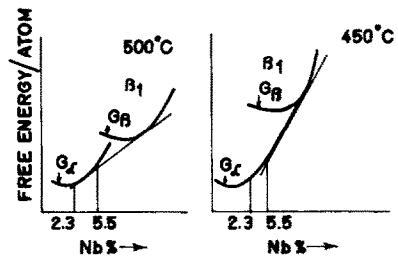

Fig. 9. Hypothetical free energy-composition diagrams at 500° and 450°C.

that for the latter. The precipitation of the β_1 phase would also be favoured from the point of view of the growth kinetics as the extent of the long range transport of niobium atoms required for the growth of a β_1 precipitate is much smaller than that in the case of a β_2 precipitate.

This metastable β_1 phase has a tendency to transform into a mixture of the α and the β_2 phases, but such a transformation would again encounter a large free energy barrier ($\Delta G_{\beta_1\beta_2}$ as shown in fig. 8(a)) and would consequently be extremely sluggish. Aldridge and Cheadle [16] have shown that the β_1 phase does not decompose even during the furnace cooling of a Zr-2.5% Nb alloy sample from the $\alpha + \beta$ phase field.

On tempering at 550°C, the Zr-5.5% Nb as well as the Zr-2.3% Nb alloys were found to behave in a similar fashion because the T_0 temperatures for both of these were above the tempering temperature. The formation of the β_1 precipitates in preference to the β_2 precipitates could be explained on lines similar to those followed in discussing the tempering behaviour of the Zr-2.3% Nb alloy at 600°C.

The precipitation of the β_1 phase would be thermodynamically impossible if the free energy corresponding to the mixture of the α and the β_1 phases were to exceed that of the supersaturated α' phase. This could happen at lower temperatures where the common tangent to the G_α and G_{β_1} curves touches the G_α curve at a composition level higher than the α' composition. It appears from the present experimental results that the common tangent touches the G_α curve at a composition X, where X lies between 2.3 and 5.5% Nb at 500° C and above 5.5% Nb at 450°C (fig. 9). In such a situation the equilibrium β_2 phase would directly precipitate out during tempering.

4.2. *Twin-boundary precipitation*

It has been mentioned earlier that a β_1 precipitate forming at a twin boundary maintains equivalent orientation relations with the two adjacent twin-related crystals. This is possible since a $\{110\}_{\beta_1}$ type mirror plane is parallel to a $\{10\bar{1}1\}_\alpha$ type twin plane. The plate shaped precipitates were seen lying along the twin plane with their flat faces, $(110)_{\beta_1}$, parallel to the twin interface. This is schematically shown in fig. 10. For this particular variant of the orientation relation, the two orthogonal directions $[11\bar{2}0]_\alpha$ and $[1\bar{1}02]_\alpha$ are parallel to the $[1\bar{1}1]_{\beta_1}$ and the $[\bar{1}12]_{\beta_1}$ directions respectively. In order to make an estimate of the degree of misfit at the precipitate-matrix interface, the repeat distances along these directions are compared in table 1. It is evident from these values that mismatch between the $(\bar{1}101)_\alpha$ and the $(110)_{\beta_1}$ planes is quite small and thus the interface separating these two planes is coherent to a reasonable extent. Since a precipitate has equivalent orientation relations with both the twin components, the same degree of coherency is maintained on both the flat faces of the plate shaped precipitate. For such a condition the surface energy requirement for nucleation would be very small and thus those variants of the Burgers' relation in which a $\{110\}_{\beta_1}$ type mirror plane lies approximately parallel to the twin interface would be predominantly operative. There can be six different orientations of the β_1 crystal which can have a $\{110\}$ type plane parallel to a given $(10\bar{1}1)$ twin plane, but these orientations are crystallographically equivalent and are not distinguishable from one another. For this reason the orientations of the β_1 precipitates nucleating separately on a set of $(10\bar{1}1)$ twins would be identical and these precipitates could join together resulting in a lamellar distribution of the β_1 phase.

The formation of the precipitate morphology along twin boundaries (fig. 11) can be explained in terms of the following growth mechanism. Since atom transfer across the coherent interface is rather slow, the thickening of a twin boundary precipitate would occur at a slow pace. In contrast, the growth of these precipitates along their habit plane would be accomplished by absorption of new atoms at the precipitate edge and this would be facilitated by a process consisting of the diffusion of solute atoms towards the twin interface followed by a short circuit diffusion along the twin boundary. As a result, thin plate shaped precipitates would form at the twin interface. In some instances, where the successive twin interfaces are closely spaced, precipitates of identical orientation, growing from adjacent twin boundaries may join and thereby produce a non-coherent boundary between the precipitate and the twin segment (fig. 11c). A sidewise movement of this incoherent interface would result in a further growth of the precipitate at the expense of the twin segment. Finally the precipitate would occupy a portion of the twin segment, with the coherency be-

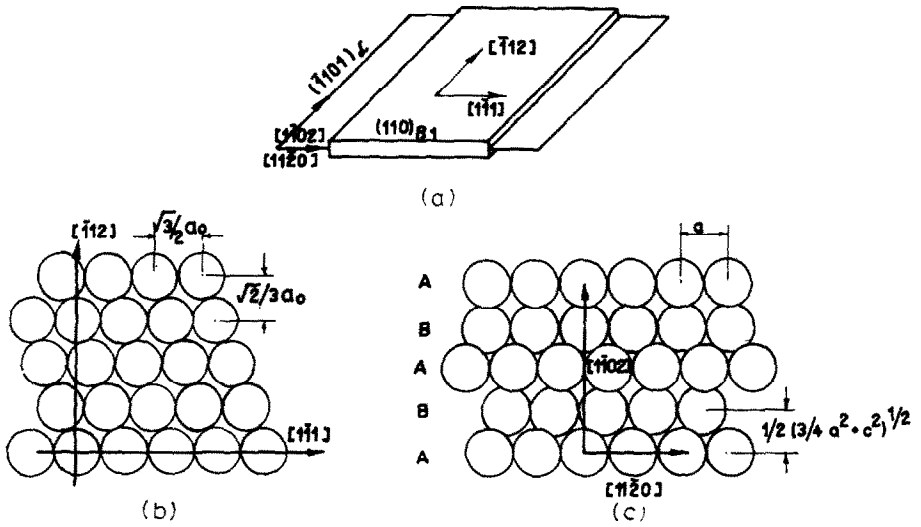

Fig. 10. (a) A schematic diagram showing the geometry of a plate shaped precipitate along $(\bar{1}101)_\alpha$ twin plane. The chosen variant of orientation relation:

$$(0001)_{\alpha_M} \| (011)_\beta;\ [11\bar{2}0]_{\alpha_M} \| [1\bar{1}1]_\beta$$

is the same as that shown in fig. 6. (b) Hard sphere model of the $(110)_\beta$ plane. Centres of all the spheres are lying on the plane of the paper. (c) Hard sphere model of the $(\bar{1}101)_\alpha$ plane. Centres of the spheres lying along alternate close packed rows are placed above and below the plane of the paper.

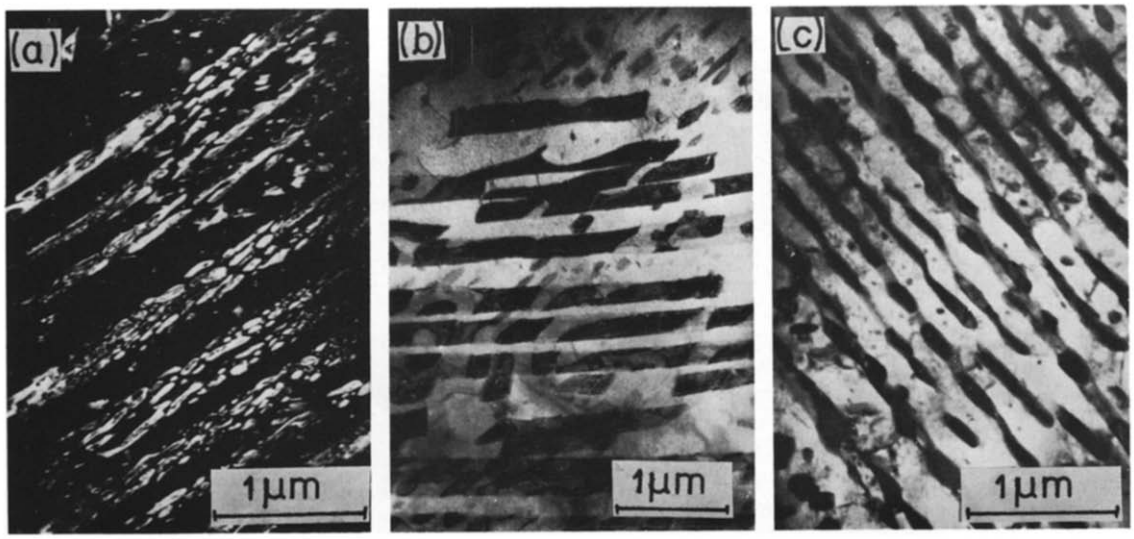

Fig. 11. Morphology of precipitates along twin boundaries. (a) Zr-5.5% Nb, beta quenched, tempered at 500°C for 100 min. Dark field micrograph showing discrete precipitates along twin boundaries. (b) Zr-2.3% Nb, beta quenched, tempered at 600°C for 10 min. Thin sheet like precipitates along the twin interfaces appear to have grown by agglomeration of discrete precipitates. (c) Zr-5.5% Nb, beta quenched, tempered at 550°C for 100 min. Micrograph shows precipitates nucleating at adjacent twin interfaces join up and grow at the expense of the twin segment. Volume fraction of the 'edge on' precipitates is 24%.

Table 1
Degrees of misfit at the interface between the $(\bar{1}101)_\alpha$ and the $(110)_{\beta_1}$ planes

	α-Zr	β_1(Zr-20% Nb)	β_2(Zr-85% Nb)	Misfit for β_1	Misfit for β_2
Interatomic distances and degrees of misfit along $[\bar{1}\bar{1}1]_\beta \parallel [11\bar{2}0]_\alpha$	a = 3.22 Å	$\sqrt{3/2}\,a_0$ = 3.05 Å	2.91 Å	5.3%	9.7%
Distance between consecutive close packed rows and degrees of misfit along $[1\bar{1}02]_\alpha \parallel [\bar{1}12]_\beta$	$\frac{1}{2}(\frac{3}{4}a^2 + c^2)^{\frac{1}{2}}$ = 2.81 Å	$\sqrt{2/3}\,a_0$ = 2.87 Å	2.73 Å	2.1%	2.8%

tween the precipitate and the matrix across the $\{10\bar{1}1\}_\alpha$ and the $\{110\}_{\beta_1}$ planes still being maintained.

Acknowledgements

The authors are thankful to Dr. M.K. Asundi, Head of the Physical Metallurgy Section, B.A.R.C. and Prof. P.R. Dhar, Head of the Materials Science Centre, IIT, Kharagpur for many valuable discussions. They are grateful also to Dr. V.K. Moorthy, Head of the Metallugy Group, B.A.R.C., for his keen interest and encouragement during the course of these investigations.

References

[1] C.D. Williams and R.W. Gilbert, J. Nucl. Mat. 18 (1966) 161.
[2] G.P. Sabol, J. Nucl. Mat. 34 (1970) 142.
[3] R.F. Heheman, Canad. Met. Quart. 11 (1972) 201.
[4] C.E. Lundin and R.H. Cox, Proc. USAEC Symp. on Zirconium Alloy Development, GEAP 4089, 1, 9–0, 1962.
[5] D.L. Douglass, The metallurgy of zirconium, Atomic Energy Review, supplement (IAEA, Vienna (1971) p. 165.
[6] B.A. Rogers and D.F. Atkins, J. Metals 7 (1955) 1034.
[7] A.G. Knapton, J. Less Com. Metals 2 (1960) 113.
[8] K.A. Bywater and J.W. Christian, Phil. Mag. 25 (1972) 1275.
[9] W.G. Burgers, Physica 1 (1934) 561.
[10] P.N.J. Flewitt, Acta Met. 22 (1974) 47–80.
[11] L. Kaufman, Acta Met. 7 (1959) 575.
[12] D. Swart, B.A. Hatt and J. Roberts, J. Appl. Phys. 16 (1965) 1081.
[13] H.K. Hardy and T.J. Heal, Prog. In Met. Phys. 5 (1954) 1.
[14] J.W. Christian, Theory of transformations in metals and alloys, (Pergamon, Oxford, 1965) p. 606.
[15] R. Becker, Z. Metallk, 29 (1937) 243; 32 (1938) 128.
[16] S.A. Aldridge and B.A. Cheadle, J. Nucl Mat. 42 (1972) 32.